Jurnal Teknologi

Full paper

Review of Brain Lesion Detection and Classification using Neuroimaging Analysis Techniques

Norhashimah Mohd Saad[a], Syed Abdul Rahman Syed Abu Bakar[b*], Ahmad Sobri Muda[c], Musa Mohd Mokji[b]

[a]*Faculty of Electronics and Computer Engineering, Universiti Teknikal Malaysia Melaka, 76100 Hang Tuah Jaya, Melaka, Malaysia*
[b]*Faculty of Electrical Engineering, Universiti Teknologi Malaysia, 81310 UTM Johor Bahru, Johor, Malaysia*
[c]*Radiology Department, Universiti Kebangsaan Malaysia Medical Centre, 56100 Cheras, Kuala Lumpur, Malaysia*

*Corresponding author: syed@fke.utm.my

Article history

Received : 25 March 2015
Received in revised form : 11 April 2015
Accepted : 13 April 2015

Graphical abstract

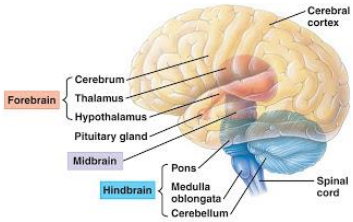

Abstract

Neuroimaging plays an important role in the diagnosis brain lesions such as tumors, strokes and infections. Within this context, magnetic resonance diffusion-weighted imaging (DWI) is clinically recommended in the differential diagnosis of several brain lesions by providing detailed information regarding lesion based on the diffusion of water molecules. Conventionally, the differential diagnosis of brain lesions is performed visually by professional neuroradiologists during a highly subjective, time-consuming process. In response, computer-aided detection/diagnosis (CAD) has become a major topic of research and, in light of novel image processing techniques, has become a widespread, possibly indispensable tool for accurate diagnosis and reduce the time required. The objective of this review is to show the recent published techniques and state-of-the-art neuroimaging techniques for the human brain lesions. The review covers neuroimaging modalities, magnetic resonance imaging, DWI and analysis techniques for CAD in detecting and classifying of brain lesion.

Keywords: Brain lesion; medical imaging; computer-aided diagnosis; segmentation; classification

Abstrak

Pengimejan neuro memainkan peranan penting dalam mendiagnosis lesi otak seperti tumor, strok dan jangkitan. Dalam konteks ini, pengimejan magnetik resonan pemberat-resapan adalah disyorkan secara klinikal dalam mendiagnosis beberapa lesi otak dengan memberikan maklumat terperinci berkenaan perbezaan jelas lesi ke atas resapan molekul air. Secara konvensional, perbezaan diagnosis lesi otak dilaksanakan secara visual oleh pakar neuroradiologi professional dengan proses subjektif dan memakan masa yang tinggi. Sebagai tindak balas, diagnosis berbantukan komputer telah menjadi topik utama kajian dan, teknik pemproses imej yang novel, telah berkembang, menjadi alat yang mungkin tidak boleh diketepikan untuk diagnosis yang jitu dan mengurangkan masa yang diperlukan. Tujuan kajian ini adalah untuk menunjukkan teknik-teknik terkini yang telah diterbitkan dan keadaan seni teknik neuroimaging untuk lesi otak manusia. Kajian ini meliputi teknik-teknik pengimejan neuro, pengimejan magnetik resonan, pengimejan pemberat-resapan dan teknik analisis untuk diagnosis berbantukan komputer dalam mengesan dan mengklasifikasi lesi otak.

Kata kunci: Lesi otak; pemprosesan imej medical; diagnosis bantuan komputer; segmentasi; klasifikasi

© 2015 Penerbit UTM Press. All rights reserve

1.0 INTRODUCTION

The human brain is the most fascinating and complex machine in the human's body is composed of hundreds of billions of neurons that inspired a great deal of study the organ. Some of the major functions of the human brain are to control muscles, coordinate body movement, sensory perceptions, memory, learning, speech, emotions, intelligences and consciousness [1].

Brain organ is made of three major parts which are the forebrain, midbrain, and hindbrain. There are four main regions of the brain which are left and right cerebrum, diencephalon, brain stem (midbrain, pons, and medulla oblongata) and cerebellum [2, 3]. The major parts, compositions and cavities of the brain are shown and listed in Figure 1.

Cerebrum (cerebral cortex) is the major part of the human brain that accounts for about 80% of its total mass. The cerebrum is divided into frontal, parietal, temporal and occipital lobes, where each area has its own functionality such as controlling speech, smell, hearing, vision, memory, complex learning or behavioral responses [1].

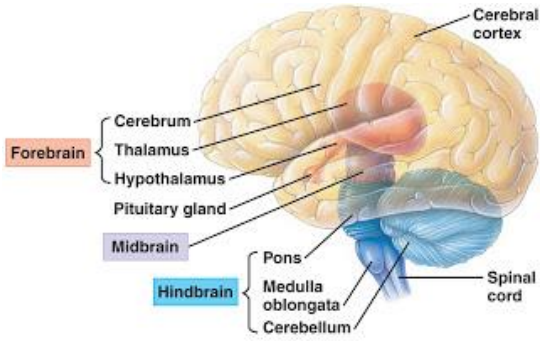

Figure 1 Major parts of the human brain [1]

It consists of grey and white matter tissue (GM/WM) and cerebral spinal fluid (CSF) in its cavity. WM consists mostly of glial cells and myelinated axons that transmit signals between the cerebrum and mid brains. GM contains most of the neurons, dendrites and capillaries. CSF is a fluid that flow from the brain's ventricles to the whole central nervous system. Any injuries or damaged brain tissue in any part of the cerebrum will subsequently deteriorates its functionality [2, 4].

Tumor, stroke and infection are lesion that may affect in the brain cerebrum. In July 2012, it was reported that cancer and stroke remain as the third and fourth leading cause of death in Malaysia [5] respectively. According to the World Health Organization (WHO), cancer and stroke have become the second and third leading cause of death worldwide after heart disease. In the United States, cancer remains the second most common cause of death with an estimated number of death caused by brain cancers at about 14,320 patients a year. The estimated number of new brain cancers is increasing from 17,000 in 2009 to 23,380 in 2014, while stroke affects nearly 750,000 new cases per year [6-8]. Hence, brain imaging plays an important role in detecting, surgery, monitoring the lesion's growth and radiation therapy planning.

■2.0 NEUROIMAGING TECHNIQUES

Development of neuroimaging technology has been rapidly evolved in the last 35 years. Beginning with the discovery of X-ray, the progress has been made further with the development of computerized tomography (CT) to the latest imaging paradigm, nuclear magnetic resonance imaging (MRI). Figure 2 shows the electromagnetic energy that is important to the development of medical imaging. The electromagnetic frequencies are measured in hertz (Hz) and the quantum electromagnetic energy is expressed in units of electron volts (eV).

The history of the development of imaging started with plain X-rays radiography, in 1895 discovered by Wilhelm Roentgen. Harvey Cushing, in 1896 was the first neurosurgeon that used X-ray for the diagnosis of diseases of the head [10]. However, X-ray radiography uses an ionized electromagnetic radiation, where the photons range from 10 keV to 150 keV, which gives highly radiation exposure to the human body. Brain consists of soft tissue in which the atom does not permit X-ray photons to pass through it as good as in bones. Therefore, X-ray provides less details of soft tissue image, and only suitable for certain brain injuries [11].

Computerized tomography or CT scanner is utilizing the idea of tomographic reconstruction principles of digital X-rays. It was first discovered by Hounsfield, in 1973 [11, 12]. During the scanning, the cross section is probed with X-rays from various directions, and the attenuated signals are converted to projections of linear attenuation. The final images of slices are reconstructed from the large separated digital X-rays projection measurement mapping into 3D projection. It can provide information about brain tissues. This improvement makes CT imaging suitable for initial assessment of brain injuries because it is faster and economical compared to other advanced imaging technology such as magnetic resonance imaging (MRI) and position emission tomography (PET) [13].

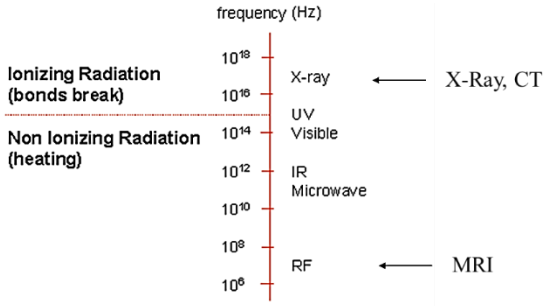

Figure 2 Electromagnetic radiation spectrum in medical imaging [9]

2.1 Magnetic Resonance Imaging

In 1973, Paul C Lauterbur and Peter Mansfield discovered the magnetic resonance imaging (MRI) as an advanced imaging modality in medicine [14, 15] . MRI is based on the theory of nuclear magnetic resonance (NMR), where the quantum physics theory behind it was discovered by Bloch and Purcell in 1946 [10, 16]. Compared to all other imaging modalities, such as CT, MRI provides superior contrast and accurate information about soft anatomy for different brain tissues. Thus, it is the best choice when soft tissue delineation is necessary. MRI helps to diagnose brain tumor and other lesions due to its high soft tissue contrast [17-20]. Images obtained by MRI are also used for analyzing and studying the behavior of the brain. For that, MRI is considered to be the best technique for neuroimaging studies [21].

The main advantages of MRI can be summarized as below [6, 22]:

- Excellent soft tissue contrast with high spatial resolution.
- Display of several images and oblique cuts.
- No harmful ionizing radiation.
- Direct multi-planar imaging – coronal, sagittal and transversal (axial) planes.
- Painless and non-invasive technique can be performed without contrast.

MRI uses a strong magnet and radiofrequency (RF) waves to provide clear and detailed pictures of internal organs and tissues. MRI machines deal with very tiny particles of hydrogen nuclei (H^+) of water molecules (H_2O), because water constitute 70% of human body. The nuclei have a quantum physics property called spin, [16] which they can be oriented in certain angles. Each nucleus rotates around its own axis. When the nuclei are exposed to a strong magnetic field, B_o, their axes are line up randomly in the direction or opposition of the magnetic field. Their precession frequency of the spin is defined by the Larmor equation [23], measured in MHz, while the external magnetic field strength, B_o is measured in Teslas (T). Common magnetic field strength is 1.5T, or 3T where higher magnetic field strength will give higher signal to noise ratio (SNR)

resulting in a better image quality. Figure 3 shows a basic schematic diagram of an MRI machine.

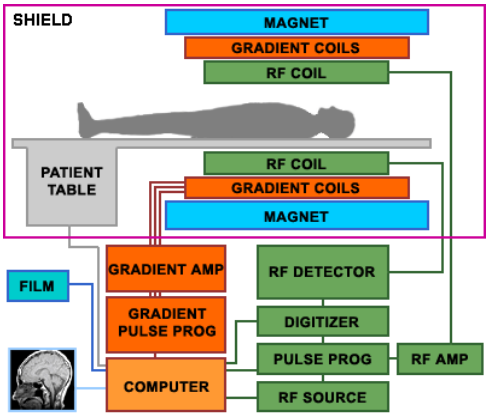

Figure 3 Schematic diagram of an MRI machine [24]

When a radio frequency (RF) pulse from the MR RF coil emits energy at the resonance frequency of the nuclei, the RF excitation irritates the nuclei's net magnetization vector (NMV) to flip. When the RF pulse is turn off, the NMV returns to the original axes and releases high energy excess in the form of waves and induces a current in the receiver coil. At this time, the system is no longer being forced out of equilibrium by the RF excitation. This process is called as T_1 recovery (T_1 relaxation times) and T_2 decay. A computer can turn those signals into an image. Different tissues have different times for T_1 recoveries and T_2 decays.

Gradient coils modify the strength of the magnetic field along the patient so as the MRI machine can scan the body in sections. Three orientations are used, which are gradient -x, -y and -z to select the orientation of the images in coronal, sagittal or axial plane. By changing the frequency of the RF coil, the MRI machine can look for the hydrogen nuclei slice by slice in the patient's body at a time.

Repetition time (TR) is the time between the applications of an RF pulse to the next RF pulse, while echo time (TE) is the time between the applications of the RF pulse to the peak of the echo signal induced in the receiver. A short TR and short TE will result in a T_1 -weighted image (T_1 recovery), while a long TR and long TE will result in a T_2 -weighted image (T_2 decay). A long TR and short TE will create a proton density (PD) image. T_1-weighted images is applied to depict the anatomy, T_2-weighted images is used for demonstrating pathology, while PD-weighted images depict both the anatomy and the disease entity based on the quantity of the nuclei [22, 23]. Figure 4 shows the images in axial plane of the difference MRI images for the same patient with tumor. CT image of the same patient is also included to show the differences between CT and MRI.

2.2 Diffusion-Weighted Imaging

The development in both hardware and software in MRI has been rapidly evolved, becoming faster, more specific and more precise [23, 25]. The latest advanced techniques include diffusion-weighted imaging (DWI), magnetic resonance spectroscopy (MRS), diffusion tensor imaging (DTI), functional MRI (fMRI) and perfusion-weighted imaging (PWI) [25-29]. Diffusion-weighted imaging (DWI) is based on the random Brownian motion of water molecules, where the theory was first described by Stejskal-Tanner [30, 31]. With DWI, the rate between rapid diffusion (unrestricted diffusion) and slow diffusion of protons (restricted diffusion) can be distinguished [23].

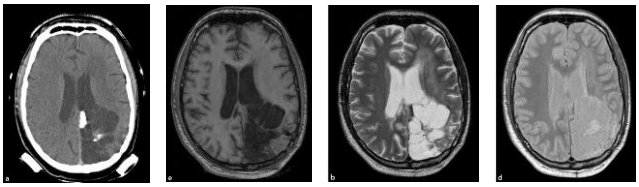

Figure 4 CT and conventional MRI of patient with tumor; (a) CT imaging, (b) T1-weighted MRI, (c) T2-weighted MRI, (d) PD-weighted MRI [25]

To obtain DWI, two equal gradient pulses are applied to the original pulse sequence used to obtain T_2-weighted imaging [32, 33]. The first gradient pulse dephases both moving and static spinning nuclei, and the second gradient rephases only the static spins. In other words, if no net movement of the spinning nuclei occurs between the gradient pulses (static molecules), the first gradient pulse dephasing the spins and the second gradient rephasing the spins. Existence of high signal intensity shows a restricted diffusion (Figure 5). If net movement of spins occurs between the gradients (moving molecules), the protons are only effected by the dephasing gradient, but not rephasing which resulted in low signal intensity.

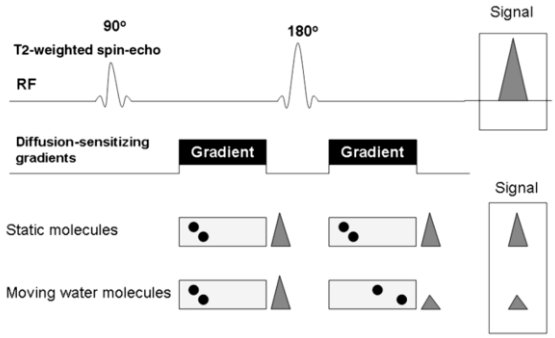

Figure 5 DWI pulse sequence [34]

DWI measures the strength of molecular motions of diffusion within a tissue structure or boundaries of white and gray matter brain tissues (WM/GM), cerebral spinal fluid (CSF) and brain lesions which have their own diffusion criteria and can be restricted by the diseases. Image contrast depends on the diffusivity, where lesion or tissues with high diffusion (watery tissues) appears dark (hypointense), and low diffusion appears bright (hyperintense) [33, 35]. The underlying equation of the DWI intensity can be written as $S = S_0 e^{-bD}$ where S is the observed image, S_0 is signal intensity without the diffusion gradient, i.e. a T_2-weighted image, D is called the diffusion coefficient where it is a measure of the strength or velocity of the micro-molecules diffusion in tissue [33, 36]. The stronger the diffusion, the greater the diffusion coefficient [36]. Lastly, b is the diffusion gradient value that is measured in s/mm^2. The b-value identifies the measurement's sensitivity to diffusion and determines the strength of the diffusion gradients. Varying the b-value generates different contrast for the same tissue. The scan obtained with b=0 s/mm^2 is a standard T_2-weighted image or zero diffusion gradient [37].

As the *b* value increases, sensitivity to the effects of diffusion increases where it serves to improve the contrast of the lesion as compared to normal tissue. However, at the same time it degrades the SNR and further image distortion [37]. The SNR of the resulting scan is compromised by increasing the echo time (TE). DWI is typically performed by using three *b*-values, usually 0, 500 and 1000 s/mm^2 to allow the calculation of apparent diffusion coefficient (ADC) image. ADC image is useful for eliminating T_2 shine-through artifacts which is a very bright pixels from T_2-weighted image that may appear bright in DWI but not associated with any lesion [31]. Figure 6 shows images of acute stroke as seen on T_2–weighted and DWI. The lesion is clearly hyperintense (red arrows) in the DWI as opposed to conventional T_2-image, the image appears normal.

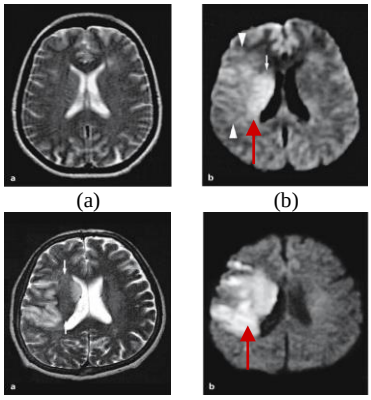

Figure 6 Acute stroke as seen on (a) T2 –weighted and (b) DWI after two hours onset ; (c) T2 –weighted and (d) DWI after 24 hours onset [31]

DWI has proven to be useful for evaluating of many brain lesions such as stroke, tumor and abscess, and many other diseases of the central nervous system. It provides higher lesion contrast compared to the conventional MRI. It has been proven valuable in distinguishing brain abscess from necrosis and tumor, as these two lesions can have intensity overlap and difficult to differentiate in conventional MRI [38, 39].

In acute infarction, changes in DWI may be revealed as early as 2 minutes after onset, whereas it may take six to twelve hours to appear in conventional MRI [25, 31, 40]. In addition, the conventional MRI and CT have sensitivities below 50% to detect infarcts within 6 hours [31], in comparison to DWI with reported sensitivities within 90–100% [25]. Thus, DWI is considered as the most sensitive brain imaging technique for earliest signs of acute ischemic stroke and hemorrhagic stroke [6, 29, 41]. DWI is also useful in giving detail components of the lesion [6, 33, 40, 42]. Overall comparisons of reliability between DWI and conventional MRI and CT imaging are summarized in Table 1. The specific purpose of neuroimaging techniques can be summarized in the flowchart in Figure 7.

2.3 Brain Lesion Diagnosis

Stroke, tumor and infection are the major brain lesion that will be discussed in this section. Stroke is a disease which affects vessels that supply blood to the brain. Stroke occurs when a blood clot blocks or brain vessel ruptures resulting in lack of oxygen supply to brain cells in the blood vessel. Due to loss of oxygen, nerve cells in the affected brain area are not able to perform basic functions which lead to the death of the brain tissue which results in brain damage. The ischemia or infarct can be due to blood clotting (thrombosis, arterial embolism), or hemorrhage due to bleeding, which both require opposite treatments.

Key diagnosis and treatment planning is obtained from MRI sequences including DWI, contrast enhanced perfusion weighted imaging (PWI) and pre/post-contrast MR angiography (MRA). The most important goal of acute stroke imaging is to assess early signs of acute stroke and to rule out hemorrhage. Moreover, it is to assess tissue with risk of dying if ischemia continues [43].

CT has been used in emergency room due to its accessibility and lower in cost [13, 44, 45]. However, the signs of stroke is difficult to detect in the first 24 hours of the onset of ischemic stroke [45]. Conventional MRI is more sensitive and more specific than CT for the detection of acute stroke for the first few hours. DWI, on the other hand has the ability to show areas of brain ischemia within minutes after onset. Figure 8 shows the accuracy in different modalities for neuroimaging of acute stroke [46]. It is clearly shows that both CT as well as conventional MRI have sensitivities below 50% with regard to detection of infarcts in the early stage, as illustrated in Figure 8.

Table 1 Comparisons of reliabilities in neuroimaging modalities

METHOD	MECHANISM	OUTCOME	SPATIAL RESOLUTION	ADVANTAGES	LIMITATIONS
CT Imaging	Ionized X-ray photons emitted with atoms of body tissue	Pixel-by-pixel map of X-Ray attenuated signals	< 0.35 mm	Provides very accurate details of bony structures. Fast acquisition.	Highly radiation exposure. Less details for soft tissue.
MRI T_1/T_2 /PD Imaging	Relaxation of excite hydrogen nuclei in a strong magnetic field	Structural images of the brain showing the anatomy and pathology.	< 1 mm	High spatial resolution of soft tissue contrast. Do not emit ionizing radiation.	Indicates areas of GM/WM soft tissue contrast but does not reflect their functional connectivity. Slow acquisition.
MRI Diffusion Imaging	Relaxation of excite hydrogen nuclei showing diffusional anisotropies	Measures degree of diffusion of water in the brain tissue	2-3 mm	Clinical usage more relevance for differential diagnosis. Fast acquisition in less than 2 minutes. High sensitivity of pathological disease.	T_2-shine through artifacts. High SNR as diffusion gradient increases. Functional interconnectivity are still to be validated.

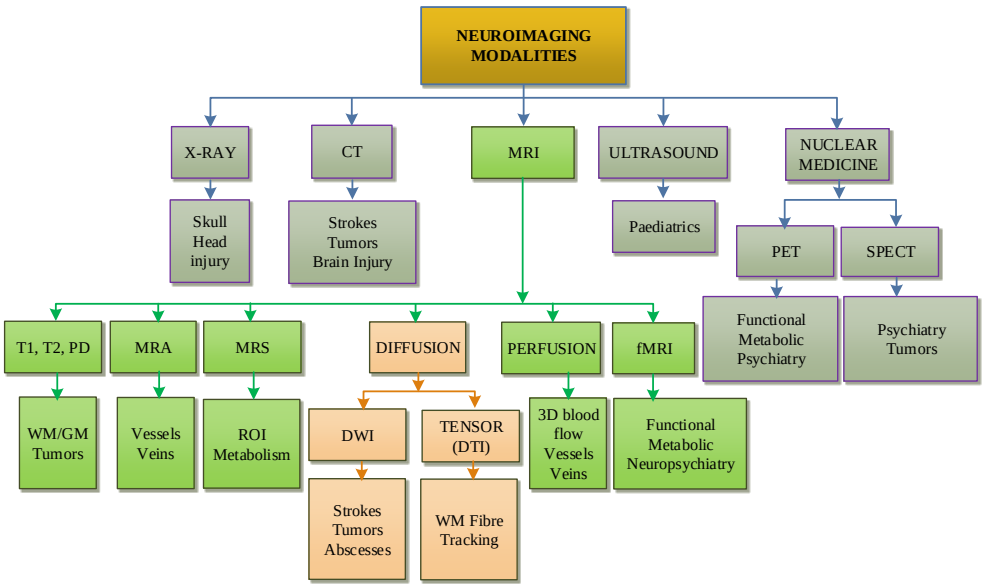

Figure 7 Neuroimaging modalities applications common use and specific purpose

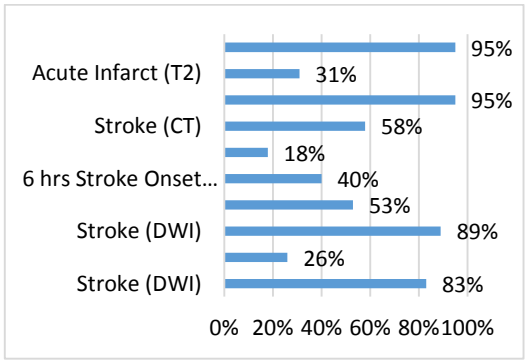

Figure 8 Average sensitivity by different modalities for neuroimaging of acute stroke [46]

Brain tumors can be defined as abnormal growths (benign or malignant) of a specific cell type that arise in the brain tissue. The WHO grading of brain tumors establishes a malignancy scale based on histologic features of the tumor. There are four histologic grades under WHO; grade I-IV which includes the lesion activity, necrosis-prone, possibility of cure and recurrence and rapid progression of the tumor cell [25].

Due to its high tissue contrast and its non-invasiveness, MRI is accepted as the most sensitive techniques to rule out brain tumors. However, conventional MRI is not specific enough to determine the histologic nature of most tumors [31]. DWI can provide more information on tumor cellularity, thereby helping in the characterization and grading of brain tumors. DWI can also has been reported to be helpful for the differential diagnosis between abscesses and cystic/necrotic brain tumors where impossible using conventional MRI [38].

Table 2 shows images of DWI in major brain lesions with diffusion coefficient of b=1000 s/mm^2 patients from Universiti Kebangsaan Malaysia Medical Centre (UKMMC). In normal brain, the region consists of brain tissue and a cavity which is full of cerebral spinal fluid (CSF) located in the middle of the brain. The DWI intensity for CSF is dark. As for brain lesions, the intensity can be divided into hyperintense and hypointense. DWI hyperintense includes acute infarction, hemorrhage, solid tumor and abscess. Chronic infarction, hemorrhage and necrosis tumor are categorized as hypointense. ADC image is the compliment to DWI, in which bright hyperintense appearance in in DWI appears dark in ADC and vice-versa.

The summary of major brain lesions, types, symptoms and pathological findings is summarized in Table 3 [18-20, 41]. High-grade solid tumors (glioma, lymphoma and metastasis; benign and malignant) typically are variable hyperintense on DWI. The common signal intensity of cystic tumor or necrosis is hypointense. The tumor's shape is commonly round, ellipse or heterogeneous lesion with mild or blur texture. Brain abscess is a lesion with inflammatory and pus due to bacterial or viral infection. Central small abscess may be seen as high signal on DWI.

Infarction is classified as acute (less than 2 weeks) and chronic (3 weeks to 3 months), each having its abnormality characteristic as shown in the table. Infarction is brain tissue damage due to vascular occlusion or blockage. Hemorrhage represents bleeding outside of the cerebral vascular. In the early stage of acute hemorrhage, the oxygenated blood product will be seen as hyperintense due to the high concentration of blood product. The DWI demonstrates hypointense for chronic hemorrhage created by deoxyhemoglobin blood products [31].

Table 2 Brain lesion appearance in DWI and ADC image

DWI	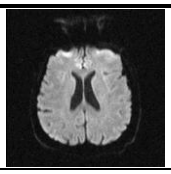	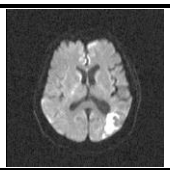	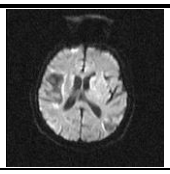	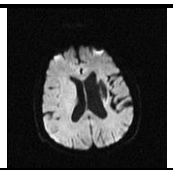
ADC	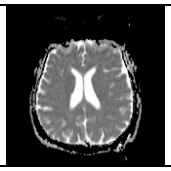	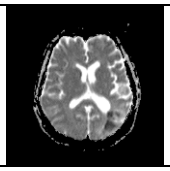	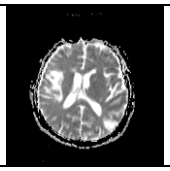	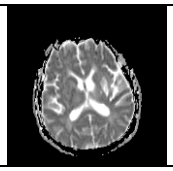
	Normal	Acute stroke	Chronic stroke	Chronic hemorrhage
DWI	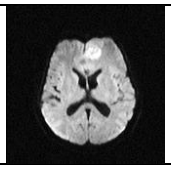	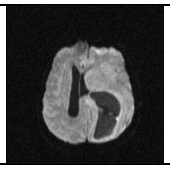	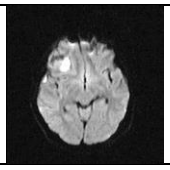	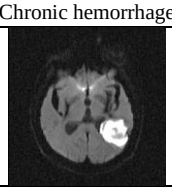
ADC	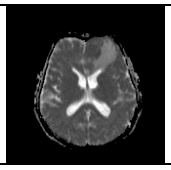	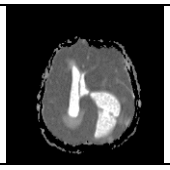	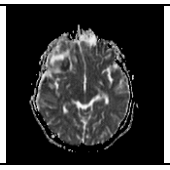	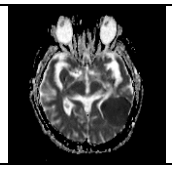
	Solid tumor	Necrosis tumor	Abscess	Acute hemorrhage

Table 3 Summary of brain lesion types, symptoms and pathological findings in DWI [18-20, 41]

Brain Lesion	DWI Image	Lesion Characteristics	Symptoms	Pathological Findings
Tumor	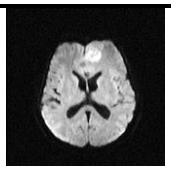 Solid tumor Necrosis tumor	**Solid:** Hyperintense **Cystic/ Necrosis:** Hypointense	Loss of balance; walking, visual and hearing problems; headache; nausea; vomiting; unusual sleep; seizure	Abnormal growth of cells in uncontrolled manner **shape:** round, ellipse, irregular **texture:** clear, partially clear, blur
Infarction (Stroke/ Ischemia)	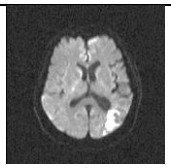 Acute infarction 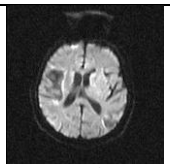 Chronic infarction	**Acute** (30 minutes - 72 hours after onset): Hyperintense **Chronic** (after 2 weeks): Hypointense	Paralysis; visual disturbances; speech problems; gait difficulties; altered level of consciousness	Cerebral vascular occlusion/ blockage
Hemorrhage (Bleeding/ Ischemia)	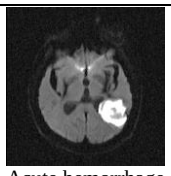 Acute hemorrhage 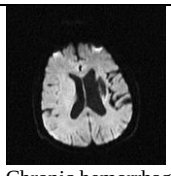 Chronic hemorrhage	**Deoxyhemoglobin:** Hyperintense **Oxyhemoglobin:** Hypointense	Paralysis; unconsciousness; visual disturbances; speech problems	Presence of blood products outside of the cerebral vascular
Infection (Abscess)	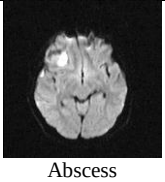 Abscess	Hyperintense	Fever; seizure; headache; nausea; vomiting; altered mental status	Bacterial, viral or fungal infections, inflammatory and pus

■3.0 COMPUTER-AIDED DIAGNOSIS TECHNIQUES FOR BRAIN LESIONS

Computer-aided diagnosis (CAD) in medical imaging has made a fast progress in the last decade. To date, the only CAD system that is has been approved by the U.S. Food and Drug Administration (FDA) is the one that is related to mammogram [47, 48], while CAD systems for human brain MRI images are yet to be approved [22]. CAD can enhance the diagnostic capabilities of physicians and reduce the time required for accurate diagnosis. The main idea of CAD is to assist radiologists in interpreting medical images by using dedicated computer systems to provide second opinion or clinical validation. Studies on CAD systems and technology show that CAD can help to improve diagnostic accuracy of radiologists, lighten the burden of increasing workload, reduce cancer misdetection and improve inter- and intra-reader variability [49, 50]. CAD research in brain MRI are includes detection of abnormalities of aneurysms in magnetic resonance angiography (MRA) images [51], Alzheimer's disease [52], multiple sclerosis [17, 53], and multimodal MRI for tumor detection [54]. Many techniques have been proposed for various medical imaging modalities, most widely used methods are fuzzy clustering, active contour and region growing [50, 55].

3.1 Stroke Lesion Analysis Techniques

For stroke lesions from CT images, Bhadauria *et al*. [13] and Loncaric *et al*. [56] use fuzzy C-mean (FCM) clustering technique. Bhadauria *et al*. integrate the features of FCM with active contour to perform the lesion segmentation with the accuracy and overlap metrics of 84.83% and 88.84% respectively. Loncaric *et al*. utilized rule-based classification technique to label the lesion's region. Zaki *et al*. [57] propose FCM method to remove background and skull from the brain CT. Then, the intracranial structure is segmented into CSF, brain matter and hemorrhage using two-level Otsu multi-thresholding method. Lee *et al*. [58] introduce a method to extract abnormality using two-phase segmentation. In the first phase, the combination of K-means and FCM methods are used to obtain a binary image. After that, decision tree is utilized to separate between normal and abnormal regions. The experimental results show that the modified FCM is more feasible and yields satisfactory results. Segmentation by using thresholding and morphological operations followed by top-hat transform and left–right asymmetry have been proposed by Chan [59] to identify small hemorrhagic lesions. Differential from normal variants is achieved by implementing a knowledge-rule based classification system and able to detect of small hemorrhage in CT with the sensitivity of 84.4%.

Semi-automated region growing approach has been proposed by Bardera *et al*. [60] and Matesin *et al*. [61]. Matesin *et al*. use features such as brightness, area, neighborhood and position to the symmetry axis to create features for a rule-based classifier. Bardera *et al*. combine the region growing approach and level set method for segmentation of brain hematoma and edema in CT. Liao *et al*. [62] propose an automatic intracranial hematoma detection technique based on binary level set method and obtain overlap metric result of 0.88. Lee *et al* propose adaptive partial smoothing filter to detect early sign of acute stroke on brain CT [63].

An automatic method for detecting of ischemic stroke in brain CT images using segmentation, texture features and tracing midline shift algorithm has been proposed by Rajini *et al*. [44]. The ischemic stroke region extracted using K-means clustering technique while gray level co-occurrence matrix (GLCM) is used as the textural features. Using support vector machine (SVM) a classification with accuracy of 98% has been obtained. Classification of three types of stroke by using texture analysis based on CT images was proposed by Bhat *et al*. [64]. Six features were used for classification that ensemble the accuracy of 85.39% to differentiate acute stroke, chronic stroke and hemorrhage successfully. Usinskas *et al*. [65] propose a method to segment ischemic stroke region on CT by utilizing joint features from mean, standard deviation, histogram and GLCM. The presented unsupervised segmentation technique shows ability to segment ischemic stroke region. Tang *et al* [45] propose a method for early detection of ischemic stroke with small lesions using image feature characteristics. An adaptive region of interest method is generated to analyze CT images of the brain by transforming the image textures from GLCM. The sensitivity and specificity of the new CAD scheme were 93.33% and 90.3%, respectively, for the detection of ischemic stroke per subject basis.

A method to detect and classify abnormality in CT is introduced by Chawla *et al*. [66]. It uses two-level classification to detect abnormalities using features derived in the intensity and wavelet that gives 90% accuracy in detecting acute infarction, chronic infarction and hemorrhage. Przelaskowski *et al*. [67] introduce a method to detect acute ischemic stroke using wavelet. Sensitivity of ischemic stroke detection is 56.3% with preserved specificity of the decisions. Shalikar *et al*. [68] present a CAD system to classify brain CT images into hemorrhagic, ischemic and normal. The proposed CAD system applies Wavelet Packet Transform (WPT) to decompose input image into sub-images and then extract texture features from sub-images using GLCM. The proposed method is evaluated on a dataset of 90 brain CT images with classification accuracy of 90%.

Nowinski *et al*. [69] develop a stroke suite of computer aided-diagnosis (CAD) system architecture specially for handling stroke in emergency room, to facilitate speed up analysis and support decision making. The system supports the evacuation of hemorrhage by thrombolytic treatment, progression and quantification of blood clot removal and automatic segmentation of blod clot from CT time series, volume measurement, and displayed in 3D.

Only few studies have been conducted on conventional MRI for detecting of stroke lesions. For example, Shen at al. [70, 71] propose FCM clustering incorporations with spatial probability maps (SPM 5) for the detection of stroke lesions in T_1-weighted MRI. The performance of the proposed method has also been demonstrated on real lesions. The detected infarct lesions from real images in general in agreement with the real lesions based on visual inspection.

3.2 Tumor Lesion Analysis Techniques

MRI is often the method of choice when soft tissue delineation is necessary. MRI helps for diagnosis of the brain tumor. Numerous algorithms and techniques have been developed for segmenting brain tumor regions from conventional MRI images. The most common used techniques were based on FCM, region growing, fuzzy sets and hybrid [22].

BraTumIA [72] is one of the developed software that performs segmentation of healthy and tumor tissues by employing MRI sequences from conventional MRI images. Porz *et al*. evaluate preoperative MRI from 25 glioblastoma patients using BraTumIA and conclude that the results are equivalent to manual tumor delineation and segmentation by neuroradiologists [73]. Performing on the Medical Image Computing and Computer Assisted Interventions (MICCAI)

Brain Tumor Segmentation (BRATS) challenge, the best similarity indices are 0.512 (automatic) and 0.694 (semi-automatic) [54, 74]. The challenge is to compare methods using the same validation datasets, with similar input data, the type of lesion, and the state of the tumor disease which are not available previously.

A method for discriminating between metastatic and primary brain tumors on MRI using T_1 post-contrast images has been proposed by Georgiadis *et al*. [75]. They proposed a modified probabilistic neural network classifier to classify metastases, meningioma and glioma. Using this method, they achieve classification accuracy of 95.24% and 93.48% in discriminating between metastatic and primary tumors and glioma from meningioma, respectively. Ain *et al*. propose tumor detection and segmentation using discrete cosine transform and Naïve Bayesian classification [76]. Brain tumor region is finally segmented using K-means clustering. They claimed that the diagnosis accuracy is achieved at 99.64%.

Hybrid Fuzzy classifications have been applied in [77-79]. El-Dahshan *et al*. propose a classification of normal and abnormal MRI using T_2 -weighted images [77]. The features of MRI are extracted using discrete wavelet transform and reduce in dimension using principal component analysis. They manage to obtain a success rate of 98% using k-nearest neighbors (k-NN) classifier. In another development, Type-II fuzzy expert system has been proposed by Fazel to recognize tumor using post-contrast T_1-weighted MRI [79]. Possibility C-mean is used for segmentation. A hybrid segmentation method was proposed by Khotanlao *et al*. that uses both region and boundary information to detect tumors [78]. Symmetry analysis and deformable model for segmentation refinement are applied to detect tumors.

Apparently, Barnathan *et al.* compared the performance of kNN, neural network, support vector machine (SVM), and decision tree-based classification on various types of normal and diseased brain tissue [80]. T_1 and T_2-weighted MRI images are analyzed to extract the textural features. The results show that kNN achieve the best performance of all classifiers obtaining average accuracies up to 89% on a combined dataset. The main drawback of these supervised techniques is that it requires fresh training, high processing time and computational effort. SVM was also implemented by Zacharaki *et al*. for distinguishing different types of brain tumors. The accuracy, sensitivity, and specificity, assessed respectively at 87%, 89%, and 79% for discrimination of metastases from glioma, and 87%, 83%, and 96% for discrimination of high grade from low grade tumor [81].

A classification and segmentation of normal and pathological tissues of tumors from multispectral MRI of the brain was proposed by Lin *et al.* [82]. Seeded region growing segmentation is used, where fuzzy edge and fuzzy image pixel similarity are used to select initial seeds automatically. Experimental results demonstrate that their method segments multispectral MRI more effectively than the Functional MRI of the Brain Automated Segmentation (FAST) Tool, K-means and SVM methods. Dubey *et al*. applied a semi-automatic region growing segmentation for brain tumors in MRI [83]. Ibrahim et al. compare the performances of brain tumor segmentation using seed based region growing, FCM and adaptive network-based fuzzy inference system (ANFIS) in MRI. They claim that ANFIS returned the best performance for bright abnormalities segmentation, while region growing performed the best for dark abnormality [84].

FCM by modifying membership weighting of every cluster and integrating spatial information was proposed by Wang and Wang [85]. In order to reduce the noise effect during segmentation, they incorporate both the local spatial context and the non-local information into the standard FCM using dissimilarity index in place of the usual distance metric. Level set active contour is also popular by many researchers. Thapaliya *et al*. propose level set, where the thresholding based values is updated and adjusted adaptively to perform tumor segmentation [86]. The algorithm was tested on eight MRI data from the internet and compare subjectively method presented by Dubey *et al* [83]. On the other hand, Rivest-Hénault and Cheriet [87] claim that they are the first researcher that use region-based level set method for MRI segmentation from The Internet Brain Segmentation Repository (IBSR) database. Their approach is for MRI WM/GM segmentation instead of brain tumor lesion delineation.

3.3 Diffusion-Weighted Imaging Analysis Techniques

DWI has been used increasingly in the analysis of differential diagnosis such as strokes, neoplasms, multiple sclerosis, metabolic diseases and brain degenerative diseases. CAD systems for detecting, identifying and segmenting of stroke lesions have been widely explored due to their highly sensitivity in detecting early cerebral ischemic stroke. The first and earliest research in DWI has been introduced by Martel *et al*. to measure the infarct volume on DWI of stroke patients. They use Bayes theorem as the conditional probabilities and adaptive thresholding of intensity histogram to adaptively segment the infarct lesions. In cases where the automatic technique failed, manual editing of the segmented images is chosen [88]. CAD for acute stroke using DWI has been implemented by Lee *et al*. to design system which enable doctors to calculate the lesion sizes and volume [89]. Graphical user interface was designed and the lesion sizes and volume was calculated using K-means and thresholding technique.

Bhanu Prakash *et al*. propose an automatic processing of DWI in ischemic stroke by using ratio of intensity probability density functions (pdf) as a divergence measure [90]. This measure is the ratio of the pdf of the left and right hemispheres to the sum of the pdf. They achieved sensitivity and specificity of 86.34% and 99.83%, respectively and Dice statistical index of 0.72. Hevia-Montiel *et al*. [91] propose a robust segmentation technique of infarct lesion by utilizing mean shift (MS) algorithm to segment the lesion. The results achieve mean similarity index of 0.538. Saraswathy et al. propose automatic identification and segmentation of infarct lesion from DWI based on restricted region growing and refinement using level sets [92]. 15 subjects from 1.5T MRI were used with diffusion coefficient b = 1000 s/mm^2. Average Dice similarity index calculated with respect to the manually traced reference image was 67.58%.

A technique for detecting and segmenting of stroke lesions in brain DWI using multiple *b*-values, b1000, b2000 and the ADC maps is presented by Mujumdar [37]. Lesion segmentation utilizes the modified Chan-Vese approach to segment the stroke lesions. The Dice coefficient, sensitivity and specificity for stroke segmentation are 84%, 87.07% and 99.90% respectively. The method is automatic and therefore could assist the clinicians in diagnosis.

The DWI has been utilized for investigating for brain metabolic diseases in pediatrics by Mahmoodabadi *et al*. [93]. DWI images of seven metabolic diseases using 1.5T MRI scanner are analyzed and classified. The system includes pre-processing, multiresolution analysis using wavelets to denoise the image, features analysis and classification using fuzzy classifier. They achieve a sensitivity and specificity of 60% and 93.33% in detecting metabolic brain diseases.

Rathi *et al*. propose to design an algorithm for biomarkers of schizophrenia disease using DWI scanner with b value of 900 s/mm^2 [94]. Confirmations are obtained by several classifiers such as kNN, Parzen window classifier and SVM to separate 21 first-episode patients from 20 normal. The best classification accuracy obtained using kNN algorithm is with 80% specificity and 78% sensitivity out of the whole brain DWI.

Santos *et al*. [95] compare multilayer perceptron, kohonen self-organizing maps (k-SOM), FCM and radial basis function (RBF) on 1.5T synthetic DWI for diagnosis of Alzheimer disease. The training were chosen from 13th slice of each sample. Maximum number of 1000 iterations for MLP are applied, while the other methods used maximum number of 200 iterations each. Overall accuracy for MLP, k-SOM, FCM and RBF regarding to the DWI volume ratio achieved are at 88.5%, 99%, 93% and 99%, respectively.

Lu *et al*. propose a method based on expectation maximization (EM) algorithm to perform tissue segmentation on DWI, fusion with 13-directional raw diffusion-tensor imaging (DTI) and a T_2 weighted data in a specific slice [96]. The results are compared subjectively with Otsu' method performed on T_2 weighted MRI, where Otsu method over-segmented the brain grey matter tissue. They find out that the grey matter and CSF can be separated away by EM algorithm, while the white matter area can be extracted to different directional dependence tissues. Similarly, another brain tissue segmentation related to fusion of DWI/DTI data was studied by Li *et al*. [97] by employing Hidden Markov random field–expectation maximization (HMRF-EM). The average volume agreements for WM, GM and CSF over ten cases are 0.89, 0.85 and 0.94 respectively. Hadjiprocopis *et al*. [98] segment the brain tissue (WM, GM and CSF) from DWI with zero diffusion coefficient, b value of 0 s/mm^2. Clustering technique is chosen, and the segmentation results are compared with Statistical Parametric Mapping version 2 (SPM 2). However, the images used are similar to MR- T_2 weighted, with no diffusion level. Overall overview of the DWI analysis, techniques and performances for brain segmentation and classification is summarized in Table 4.

4.0 CONCLUSION

This paper review of brain lesions through neuroimaging modalities, MRI and DWI in detecting and classifying the lesions. Tumors, strokes and infections are the major brain lesions that may affect in the brain cerebrum. Brain imaging is essential for diagnosis and treatment planning. MRI is accepted as the best modality for neuroimaging studies because it provides excellent soft tissue contrast, superior resolutions and no harmful radiation as compared to other imaging modalities.

On the other hand, the development in both hardware and software in MRI has been rapidly evolved. One of the advanced MRI technique is DWI, based on the random Brownian motion of water molecules in brain tissue to measure diffusion rate. DWI has been proven as the highest sensitivity in early strokes detection and in giving details of lesion's component. Therefore, the clinical usage of DWI is more relevance for brain lesion differential diagnosis.

To implement successful therapy and treatment planning, it is necessary to detect and classify of the brain lesions. To assist visual interpretation of the medical images, CAD has become a major research subject in diagnostic radiology. Medical imaging techniques help radiologists in diagnosing the lesion. CAD can help to improve diagnostic accuracy of radiologists, lighten their increasing workload, reduce misinterpretation due to fatigue or overlooked and improve inter- and intra-reader variability. With CAD, radiologists use the computer output as a second opinion in making the final decisions.

Image analysis techniques for detecting and classifying of brain lesions has become a major research of interest. Various techniques for image segmentation, features extraction and classification are essential in developing a system and for the detection of various lesions. Many researchers have studied in this area, commonly, the target is the segmentation or classification on a single disease, such as stroke or tumor via conventional MRI or CT. The database for these modalities are also available online for research studies. However, the development of automatic and accurate system is still remains an open problem. Only few studies have been reported on DWI and no researchers are perform major brain lesions classification of real clinical DWI scans. This is due to the confidentiality of the DWI data. To date, a large dataset for DWI is not available to public.

One of the most important tasks in medical image processing is segmentation. The segmentation task involves labelling the meaningful regions in a given image. Various methods have been explored and discussed in this review. Popular methods are regions and edge based techniques, both can either be automatic and semi-automatic. Thresholding, Fuzzy clustering and region growing are the well-known methods for region based segmentation due to superior performance and less complex. Level set and active contour are among popular methods for edge based segmentation. Hybrid techniques, further refinement, and post-processing will improve the segmentation and remove the noises. Supervised classification approaches such as neural network requires fresh training each time a new data is arrived and requires high computational and processing time. The main advantage of automatic segmentation is fast respond, while for classification, the results should be convincing, low classification errors and comparable efficiency with the diagnosis done by neuroradiologists.

With the advance of computational intelligence and machine learning techniques, CAD may attracts more attentions in the new future. There are still much room to utilize other techniques and integrate them into one large system. Multimodal brain lesion segmentation that includes three dimensional analysis is another room to be explored. Further experiments and evaluations are needed to implement the system and to aid neuroradiologists. Nevertheless, this is not meant that the role of doctors and neuroradiologists will be taken over by such intelligent systems. Such systems would rather serve as a compliment for clinical validation to neuroradiologists.

Table 4 Summary of methods for DWI segmentation and classification

	Study	Methods	Input	Purpose	Dataset	Classifier	Results
1.	Mahmoodabadi *et al*. [93]	-Wavelets for filtering/denoising -Histogram thresholding (ROI)	DWI & ADC: -22 features, structural and general characteristics from DWI	Classification metabolic brain diseases in paediatric	1.5 T DWI 20 patients	Fuzzy relational classifier	Sensitivity= 60% Specificity=93%
2.	Li *et al*. [97]	HMRF-EM	DWI and DTI: (ADC, eigen value, fractional and relative Anisotropy, volume Ratio)	CSF/WM/GM classification	1.5 T DWI b_0=0 s/mm^2 10 images		Jaccard Similarity Index: WM=0.89 GM= 0.85 CSF=0.94
3.	Hevia-Montiel *et al*. [91]	Mean shift and edge confidence map as gradient estimator	DWI	Acute infarction	1.5 T DWI 15 patients		Jaccard index =0.538
4.	Hwang *et al*. [99]	Region growing	DWI	Skull stripping	3T DWI		Misclassified error: Histogram=0.6154 Snake=0.5869 Proposed=0.4234
5.	Lu *et al*. [96]	Hierarchical clustering EM algorithm	DWI / DTI	CSF/WM/GM classification	1.5 T DWI/DTI 5 normal images		Subjective evaluation comparison with Otsu's method
6.	Santos *et al*. [95]	Volume ratio of fluid-tissue rate	DWI	Alzheimer disease	1.5 T DWI 60 images of slice-13	k-SOM MLP FCM RBF	MLP=88.5% k-SOM=99% FCM=93% RBF=99%
7.	Bhanu Prakash *et al*. [90]	Divergence measure ratio of intensity PDF	DWI	Infarct Lesion i. Slice identification ii. Lesion segmentation	1.5 T DWI 57 Patients		Lesion Segmentation: Sensitivity=86.34% Specificity=99.83% Dice=0.72 Slice identification: Sensitivity=90.05% Specificity= 68.78%
8.	Martel *et al*. [88]	Adaptive thresholding	DWI	Semi-automatic Stroke segmentation	1.5 T DWI 63 patients		Misclassified error: 0.049 (high contrast) 0.1 (low contrast)
9.	Lee *et al*. [89]	Thresholding k-means	DWI	Measure volume of Acute stroke	1.5 T DWI		Comparison with expert's calculation
10.	Bhanu Prakash *et al*. [100]	Gaussian mixture model	DWI	Same as no.8.	1.5 T DWI 13 patients	Probability neural network	Sensitivity=81% Specificity=99% Dice=0.6
11.	Saraswathy *et al*. [92]	Region growing and level set refinement	DWI	Ischemic lesions	1.5 T DWI 15 images		Dice=67.58%
12.	Mujumdar [37]	Chan-Vese active contour	DWI	Stroke segmentation	1.5 T DWI 24 images		Sensitivity=87.07% Specificity=99.9% Dice=84%
13.	Rathi *et al*. [94]	Kernel based method Statistical different diffusion measure		Schizophrenia disease	1.5 T DWI b value, 900 s/mm^2 21 patients 20 normal	kNN Parzen window SVM	kNN performance: Sensitivity=78%% Specificity=80%
14	Hadjiprocopis *et al*. [98]	Clustering	DWI	Brain tissue segmentation	1.5 T DWI b value, 0 s/mm^2		Subjective evaluation with SPM 2 package

Acknowledgement

The author would like to thank Malaysia Ministry of Higher Education (MOHE) for financial assistance while conducting this research.

References

[1] N. A. Campbell, J. B. Reece, M. R. Taylor, E. J. Simon, and J. Dickey. 2009. *Biology: Concepts & Connections*. Sixth ed. vol. 3. Pearson/Benjamin Cummings.
[2] R. S. Snell. 2010. *Clinical Neuroanatomy*. 7th ed. Lippincott Williams & Wilkins.
[3] M. Rubin, J. E. Safdieh and F. H. Netter. 2007. *Netter's Concise Neuroanatomy*. Saunders Elsevier.
[4] W. L. Nowinski. 2011. Introduction to Brain Anatomy. In *Biomechanics of the Brain*. K. Miller, Ed. ed: Springer Science+Business Media. 5–40.
[5] Ministry-of-Health. 2012. Health Facts 2012. Ministry Of Health Malaysia.
[6] Siemens. 2010. Diffusion Weighted MRI of the Brain, in *MAGNETOM Maestro Class*, ed. Siemens Medical Germany: Siemens Medical Solutions That Help.
[7] American-Cancer-Society. 2009. *Cancer Facts & Figures 2009*. Available: http://www.cancer.org/research/cancerfactsstatistics/cancerfactsfigures2009/index.
[8] American-Cancer-Society. 2014. *Cancer Facts & Figures 2014*. Available: http://www.cancer.org/research/cancerfactsstatistics/cancerfactsfigures2014/index.
[9] J. T. Voyvodic. 2005. *Basic Physical Principles of MRI*: *Brain Imaging and Analysis Center*. Duke University Medical Center, Durham, North Carolina, USA.
[10] P. E. Kim and C. S. Zee. 2007. Imaging of the Cerebrum. *Neurosurgery*. 61.
[11] J. G. Webster and J. Wiley. 1999. *Wiley Encyclopedia of Electrical and Electronics Engineering*. John Wiley & Sons, Inc.
[12] C. Guy and D. Ffytche. 2005. *An Introduction to the Principles of Medical Imaging*: World Scientific.
[13] H. Bhadauria, A. Singh and M. Dewal. 2013. An Integrated Method for Hemorrhage Segmentation from Brain CT Imaging. *Computers & Electrical Engineering*. 39: 1527–1536.
[14] P. C. Lauterbur, 1973. Image Formation by Induced Local Interactions: Examples Employing Nuclear Magnetic Resonance. *Nature*. 242: 190–191.
[15] P. Mansfield. 1977. Multi-planar Image Formation using NMR Spin Echoes. *Journal of Physics C: Solid State Physics*. 10: L55.
[16] Siemens, 2010. Magnets, Spins, and Resonances: An Introduction to the Basics of Magnetic Resonance. In *Siemens Medical Solutions That Help*.
[17] E. M. Sweeney, R. T. Shinohara, N. Shiee, F. J. Mateen, A. A. Chudgar and J. L. Cuzzocreo. 2013. OASIS is Automated Statistical Inference for Segmentation, with applications to Multiple Sclerosis Lesion Segmentation in MRI. *NeuroImage: Clinical*. 2: 402–413.
[18] S. Cha, 2006. Update on Brain Tumor Imaging: From Anatomy to Physiology. *American Journal of Neuroradiology*. 27: 475–487.
[19] R. T. Ullrich, L. W. Kracht and A. H. Jacobs. 2008. Neuroimaging in Patients with Gliomas, Seminars in Neurology. 484–494.
[20] O. Kastrup, I. Wanke and M. Maschke, 2008. Neuroimaging of Infections of the Central Nervous System, Seminars in Neurology. 511–522.
[21] L. Hsu, 2005. MR Imaging of the Central Nervous System. *Minimally Invasive Neurosurgery*. ed: Humana Press Inc, Totowa, NJ.
[22] E.-S. A. El-Dahshan, H. M. Mohsen, K. Revett and A.-B. M. Salem. 2014. Computer-Aided Diagnosis of Human Brain Tumor Through MRI: A Survey and a New Algorithm. *Expert Systems with Applications*. 41: 5526–5545.
[23] R. Bitar. 2006. MR Pulse Sequences: What Every Radiologist Wants to Know but Is Afraid to Ask. *RadioGraphics*. 26: 513–537.
[24] M. B. M. Ariffanan, 2009. Medical Image Classification and Symptoms Detection using Neuro Fuzzy, Master Thesis, Universiti Teknologi Malaysia.
[25] M. Winntermark, M. D. Wirt, P. Mukherjee, G. Zaharchuk, E. Barbier, W. P. Dillon. 2008. Brain, Head and Neck. *Magnetic Resonance Tomography*. M. F. Reiser, W. Semmler, and H. Hricak, Eds. ed: Springer Berlin Heidelberg. 169–533.
[26] J. M. Provenzale, S. Mukundan and D. P. Barboriak. 2006. Diffusion-weighted and Perfusion MR Imaging for Brain Tumor Characterization and Assessment of Treatment Response 1. *Radiology*. 239: 632–649.
[27] Y. Han, E. Li, J. Tian, J. Chen, H. Wang and J. Dai, 2006. The Application of diffusion-and Perfusion-Weighted Magnetic Resonance Imaging in the Diagnosis and Therapy of Acute Cerebral Infarction, *International Journal of Biomedical Imaging*.
[28] N. Rollin, J. Guyotat, N. Streichenberger, J. Honnorat, V.-A. T. Minh, and F. Cotton. 2006. Clinical Relevance of Diffusion and Perfusion Magnetic Resonance Imaging in Assessing Intra-Axial Brain Tumors. *Neuroradiology*. 48: 150–159.
[29] S. J. Holdsworth and R. Bammer. 2008. Magnetic Resonance Imaging Techniques: fMRI, DWI, and PWI, Seminars in Neurology. 395.
[30] E. Stejskal and J. Tanner. 1965. Spin Diffusion Measurements: Spin Echoes in the Presence of a Time-dependent Field Gradient. *The Journal of Chemical Physics*. 42: 288–292.
[31] T. Moritani, S. Ekholm and P.-L. Westesson. 2005. Diffusion-Weighted MR Imaging of the Brain.
[32] D. Weishaupt, V. D. Köchli and B. Marincek. 2006. 7 Basic Pulse Sequences. In *How Does MRI Work? An Introduction to the Physics and Function of Magnetic Resonance Imaging*. 2nd Edition ed: Springer Berlin Heidelberg. 47–56.
[33] P. W. Schaefer, P. E. Grant and R. G. Gonzalez. 2000. Diffusion-Weighted MR Imaging of the Brain 1. *Radiology*. 217: 331–345.
[34] D.-M. Koh and D. J. Collins. 2007. Diffusion-Weighted MRI in the Body: Applications and Challenges in Oncology. *American Journal of Roentgenology*. 188: 1622–1635.
[35] D. Koh and A. Padhani, 2014. Diffusion-Weighted MRI: a New Functional Clinical Technique for Tumour Imaging.
[36] J. Graessner. 2011. Frequently Asked Questions: Diffusion-Weighted Imaging (DWI). *How I do it MAGNETOM FLASH*. 84–87.
[37] S. Mujumdar. 2013. Detection and Segmentation of Stroke Lesions from Diffusion Weighted MRI Data of the Brain, International Institute of Information Technology Hyderabad.
[38] L. Nadal Desbarats, S. Herlidou, G. de Marco, C. Gondry-Jouet, D. Le Gars, H. Deramond. 2003. Differential MRI Diagnosis between Brain Abscesses and Necrotic or Cystic Brain Tumors using the Apparent Diffusion Coefficient and Normalized Diffusion-Weighted Images. *Magnetic Resonance Imaging*. 21: 645–650.
[39] P. H. Lai, J. T. Ho, W. L. Chen, S. S. Hsu, J. S. Wang and H. B. Pan. 2002. Brain Abscess and Necrotic Brain Tumor: Discrimination with Proton MR Spectroscopy and Diffusion-weighted Imaging. *American Journal of Neuroradiology*. 23: 1369–1377.
[40] S. K. Mukherji, T. L. Chenevert and M. Castillo. 2002. State of the Art: Diffusion-Weighted Magnetic Resonance Imaging. *Journal of Neuro-Ophtalmology*. 22.
[41] M. D. Hammer and L. R. Wechsler. 2008. Neuroimaging in Ischemia and Infarction, Seminars in Neurology. 446–452.
[42] M. Saad, S. Abu-Bakar, S. Muda, M. Mokji and A. Abdullah. 2012. Fully Automated Region Growing Segmentation of Brain Lesion in Diffusion-Weighted MRI. *IAENG International Journal of Computer Science*. 39: 155–164.
[43] A. Srinivasan, M. Goyal, F. A. Azri, and C. Lum, 2006. State-of-the-Art Imaging of Acute Stroke. *RadioGraphics*. 26: 75–95.
[44] N. Hema Rajini and R. Bhavani. 2013. Computer Aided Detection of Ischemic Stroke using Segmentation and Texture Features, *Measurement*. 46: 1865–1874.
[45] F.-h. Tang, D. K. Ng, and D. H. Chow. 2011. An Image Feature Approach for Computer-Aided Detection of Ischemic Stroke. *Computers in Biology and Medicine*. 41: 529–536.
[46] J. A. Chalela, C. S. Kidwell, L. M. Nentwich, M. Luby, J. A. Butman, A. M. Demchuk. 2007. Magnetic Resonance Imaging and Computed Tomography in Emergency Assessment of Patients with Suspected Acute Stroke: A Prospective Comparison. *The Lancet*. 369: 293–298.
[47] J. J. Fenton, S. H. Taplin, P. A. Carney, L. Abraham, E. A. Sickles, C. D'Orsi, 2007. Influence of Computer-aided Detection on Performance of Screening Mammography. *New England Journal of Medicine*. 356: 1399–1409.
[48] H. Kobatake. 2007. Future CAD in Multi-Dimensional Medical Images:–Project on Multi-Organ, Multi-Disease CAD System, *Computerized Medical Imaging and Graphics*. 31: 258–266.
[49] H. Fujita, Y. Uchiyama, T. Nakagawa, D. Fukuoka, Y. Hatanaka, T. Hara. 2008. Computer-Aided Diagnosis: The Emerging of Three CAD Systems Induced by Japanese Health Care Needs. *Computer Methods and Programs in Biomedicine*. 92: 238–248.
[50] H. Fujita, J. You, Q. Li, H. Arimura, R. Tanaka, S. Sanada. 2010. State-of-the-Art of Computer-Aided Detection/Diagnosis (CAD), *Medical Biometrics*. Springer. 296–305.

[51] X. Yang, D. J. Blezek, L. T. Cheng, W. J. Ryan, D. F. Kallmes and B. J. Erickson. 2011. Computer-Aided Detection of Intracranial Aneurysms in MR Angiography. *Journal of Digital Imaging*. 24: 86–95.
[52] M. Termenon, A. Besga, J. Echeveste, A. Gonzalez-Pinto and M. Graña. 2011. Alzheimer Disease Classification on Diffusion Weighted Imaging Features. *New Challenges on Bioinspired Applications*. ed: Springer. 120–127.
[53] Y. Zhang. 2012. MRI Texture Analysis in Multiple Sclerosis. *Journal of Biomedical Imaging*. 2.
[54] B. R. Menze, M. Van and K. Leemput. 2014. The Multimodal Brain Tumor Image Segmentation Benchmark (BRATS). *IEEE Transactions on Medical Imaging*.
[55] M. A. Balafar, A. R. Ramli, M. I. Saripan and S. Mashohor. 2010. Review of Brain MRI Image Segmentation Methods. *Artificial Intelligence Review*. 33: 261–274.
[56] S. Loncaric, A. P. Dhawan, D. Cosic, D. Kovacevic, J. Broderick and T. Brott. 1999. Quantitative Intracerebral Brain Hemorrhage Analysis. *Medical Imaging*. 886–894.
[57] W. M. D. W. Zaki, M. F. A. Fauzi, R. Besar and W. S. H. M. W. Ahmad. 2011. Abnormalities Detection in Serial Computed Tomography Brain Images using Multi-Level Segmentation Approach. *Multimedia Tools and Applications*. 54: 321–340.
[58] T. H. Lee, M. F. A. Fauzi, R. Komiya and S. C. Haw. 2008. Unsupervised Abnormalities Extraction and Brain Segmentation, International Conference on Intelligent System and Knowledge Engineering. 1185–1190.
[59] T. Chan. 2007. Computer Aided Detection of Small Acute Intracranial Hemorrhage on Computer Tomography of Brain. *Computerized Medical Imaging and Graphics*. 31: 285–298.
[60] A. Bardera, I. Boada, M. Feixas, S. Remollo, G. Blasco and Y. Silva, 2009. Semi-Automated Method for Brain Hematoma and Edema Quantification using Computed Tomography. *Computerized Medical Imaging and Graphics*. 33: 304–311.
[61] M. Matesin, S. Loncaric and D. Petravic. 2001. A Rule-based Approach to Stroke Lesion Analysis from CT Brain Images, Proceedings of the 2nd International Symposium on Image and Signal Processing and Analysis. 219–223.
[62] C. C. Liao, F. Xiao, J.-M. Wong, and I. Chiang. 2010. Computer-aided Diagnosis of Intracranial Hematoma With Brain Deformation On Computed Tomography. *Computerized Medical Imaging and Graphics*. 34: 563–571.
[63] Y. Lee, N. Takahashi, D.-Y. Tsai and H. Fujita, 2006. Detectability Improvement of Early Sign of Acute Stroke on Brain CT Images using an Adaptive Partial Smoothing Filter, *Medical Imaging*, 61446Q-61446Q-8.
[64] P. Bhat and M. Singh. 2012. Classification of Stroke using Texture Analysis on CT Images. *International Journal of Soft Computing and Engineering (IJSCE)*. 2: 527–530.
[65] A. Ušinskas. 2004. Ischemic Stroke Segmentation on CT Images using Joint Features. *Informatica*. 15: 283–290.
[66] M. Chawla, S. Sharma, J. Sivaswamy, and L. Kishore. 2009. A Method for Automatic Detection and Classification of Stroke from Brain CT images, Annual International Conference of the IEEE Engineering in Medicine and Biology Society. 3581–3584.
[67] A. Przelaskowski, K. Sklinda, P. Bargieł, J. Walecki, M. Biesiadko-Matuszewska and M. Kazubek. 2007. Improved Early Stroke Detection: Wavelet-based Perception Enhancement of Computerized Tomography Exams. *Computers in Biology and Medicine*. 37: 524–533.
[68] A. Shalikar, M. R. Ashouri, and M. H. N. Shahraki, 2014. A CAD System for Automatic Classification of Brain Strokes in CT Images. *International Journal of Mechatronics, Electrical and Computer Technology*. 4.
[69] W. L. Nowinski, G. Qian, K. B. Prakash, I. Volkau, W. K. Leong and S. Huang. 2008. Stroke Suite: CAD Systems for Acute Ischemic Stroke, Hemorrhagic Stroke, and Stroke in ER, *Medical Imaging and Informatics*. Springer. 377–386.
[70] S. Shen, A. J. Szameitat, and A. Sterr, 2010. An Improved Lesion Detection Approach Based on Similarity Measurement Between Fuzzy Intensity Segmentation and Spatial Probability Maps. *Magnetic Resonance Imaging*. 28: 245–254.
[71] S. Shen, A. J. Szameitat, and A. Sterr, 2008. Detection of Infarct Lesions from Single MRI Modality using Inconsistency between Voxel Intensity and Spatial Location—A 3-D Automatic Approach. *IEEE Transactions on Information Technology in Biomedicine*. 12: 532–540.
[72] Dec 2014. *BraTumIA (Brain Tumor Image Analysis) Software*. Available: http://www.istb.unibe.ch/content/research/medical_image_analysis/software/index_eng.html.
[73] N. Porz, S. Bauer, A. Pica, P. Schucht, J. Beck, R. K. Verma, 2014. Multi-Modal Glioblastoma Segmentation: Man versus Machine, *PloS one*. 9: e96873.
[74] *MICCAI Brain Tumor Segmentation (BRATS) challenge*. Available:http://www2.imm.dtu.dk/projects/BRATS2012/.
[75] P. Georgiadis, D. Cavouras, I. Kalatzis, D. Glotsos, E. Athanasiadis, S. Kostopoulos, 2009. Enhancing the Discrimination Accuracy between Metastases, Gliomas and Meningiomas on Brain MRI by Volumetric Textural Features and Ensemble Pattern Recognition Methods, *Magnetic Resonance Imaging*. 27: 120–130.
[76] Q.-u. Ain, I. Mehmood, S. M. Naqi, and M. A. Jaffar. 2010. Bayesian Classification using DCT Features for Brain Tumor Detection. *Knowledge-Based and Intelligent Information and Engineering Systems*. Springer. 340–349.
[77] E.-S. A. El-Dahshan, T. Hosny, and A.-B. M. Salem, 2010. Hybrid Intelligent Techniques for MRI Brain Images Classification. *Digital Signal Processing*. 20: 433–441.
[78] H. Khotanlou, O. Colliot, J. Atif, and I. Bloch. 2009. 3D Brain Tumor Segmentation in MRI using Fuzzy Classification, Symmetry Analysis and Spatially Constrained Deformable Models. *Fuzzy Sets and Systems*. 160: 1457–1473.
[79] M. Fazel Zarandi, M. Zarinbal, and M. Izadi, 2011. Systematic Image Processing for Diagnosing Brain Tumors: A Type-II Fuzzy Expert System Approach. *Applied Soft Computing*. 11: 285–294.
[80] M. Barnathan, J. Zhang, E. Miranda, V. Megalooikonomou, S. Faro and H. Hensley. 2008. A Texture-based Methodology for Identifying Tissue Type in Magnetic Resonance Images. IEEE International Symposium in Biomedical Imaging: From Nano to Macro. 464–467.
[81] E. I. Zacharaki, S. Wang, S. Chawla, D. S. Yoo, R. Wolf and E. R. Melhem. 2009. MRI-based Classification of Brain Tumor Type and Grade using SVM-RFE, IEEE International Symposium in Biomedical Imaging: From Nano to Macro. 1035–1038.
[82] G.-C. Lin, W.-J. Wang, C.-C. Kang, and C.-M. Wang. 2012. Multispectral MR Images Segmentation Based on Fuzzy Knowledge and Modified Seeded Region Growing. *Magnetic Resonance Imaging*. 30: 230–246.
[83] R. Dubey, M. Hanmandlu and S. Gupta, 2009. Region Growing for MRI Brain Tumor Volume Analysis. *Indian Journal of Science and Technology*. 2: 26–31.
[84] S. Ibrahim, N. E. A. Khalid, and M. Manaf. 2010. Seed-based Region Growing (SBRG) vs Adaptive Network-based Inference System (ANFIS) vs Fuzzy C-Means (FCM): Brain Abnormalities Segmentation. *International Journal of Electrical and Computer Engineering*. 5: 94–104.
[85] P. Wang and H. Wang. 2008. A Modified FCM Algorithm for MRI Brain Image Segmentation. *Future BioMedical Information Engineering, 2008. FBIE'08*. 26–29.
[86] K. Thapaliya, J.-Y. Pyun, C.-S. Park, and G.-R. Kwon. 2013. Level Set Method with Automatic Selective Local Statistics for Brain Tumor Segmentation in MR Images. *Computerized Medical Imaging and Graphics*. 37: 522–537.
[87] D. Rivest-Hénault and M. Cheriet. 2011. Unsupervised MRI Segmentation of Brain Tissues using a Local Linear Model and Level Set. *Magnetic Resonance Imaging*. 29: 243–259.
[88] A. L. Martel, S. J. Allder, G. S. Delay, P. S. Morgan, and A. R. Moody. 1999. Measurement of Infarct Volume in Stroke Patients using Adaptive Segmentation of Diffusion Weighted MR Images. *Medical Image Computing and Computer-Assisted Intervention–MICCAI'99*. 22–31.
[89] J. D. Lee, T. C. Chang, C. H. Huang, S. J. Wu, and C. J. Chen. 2004. Computer-aided Diagnosis System for Acute Stroke Using Diffusion Weighted Images with Volume Calculation, 26th Annual International Conference of the IEEE EMBS, San Fransisco, USA. 1529–1532.
[90] K. Bhanu Prakash, V. Gupta, and W. L. Nowinski. 2010. Segmenting Infarct from Diffusion-Weighted Imaging Volume, United States Patent.
[91] N. Hevia-Montiel, J. R. Jimenez-Alaniz, V. Medina-Banuelos, O. Yanez-Suarez, C. Rosso and Y. Samson. 2007. Robust Nonparametric Segmentation of Infarct Lesion from Diffusion-Weighted MR Images, 29th Annual International Conference of the IEEE Engineering in Medicine and Biology Society. 2102–2105.
[92] S. Saraswathy, S. Sharma, D. Shanbhag, U. Patil, and R. Mullick. 2009. Automatic Identification and Segmentation of Infarct Lesions from Diffusion Weighted MR Images and ADC Maps. *International Society for* Magnetic Resonance *in Medicine*.
[93] S. Z. Mahmoodabadi, J. Alirezaie, P. Babyn, A. Kassner, and E. Widjaja. 2011. Wavelets and Fuzzy Relational Classifiers: A Novel

Diffusion-weighted Image Analysis System for Pediatric Metabolic Brain Diseases, *Computer Methods and Programs in Biomedicine*, 103: 74–86.

[94] Y. Rathi, J. Malcolm, O. Michailovich, J. Goldstein, L. Seidman and R. W. McCarley. 2010. Biomarkers for Identifying First-episode Schizophrenia Patients using Diffusion Weighted Imaging. *Medical Image Computing and Computer-Assisted Intervention*. Springer. 657–665.

[95] W. P. Santos, F. M. Assis, R. E. Souza, P. B. S. Filho, and F. B. L. Neto. 2009. Dialectical Multispectral Classification of Diffusion-weighted Magnetic Resonance Images as an Alternative to Apparent Diffusion Coefficients Maps to Perform Anatomical Analysis. *Computerized Medical Imaging and Graphics*. 33: 442–460.

[96] C.-F. Lu, P.-S. Wang, B.-W. Soong, Y.C. Chou, H.-C. Li, and Y.-T. Wu, 2009. Multi-tissue Classification of Diffusion-Weighted Brain Images in Multiple System Atrophy Using Expectation Maximization Algorithm Initialized by Hierarchical Clustering, 13th International Conference on Biomedical Engineering. 722–725.

[97] H. Li, T. Liu, G. Young, L. Guo, and S. T. Wong. 2006. Brain Tissue Segmentation Based on DWI/DTI Data, 3rd IEEE International Symposium on Biomedical Imaging: Nano to Macro. 57–60.

[98] A. Hadjiprocopis, W. Rashid, and P. S. Tofts, 2005. Unbiased Segmentation of Diffusion-weighted Magnetic Resonance Images of the Brain using Iterative Clustering. *Magnetic Resonance Imaging*. 23: 877–885.

[99] J. Hwang, Y. Han, and H. Park. 2007. Segmentation of Brain Parenchyma using Bilateral Filtering and Region Growing, 29th Annual International Conference of the IEEE Engineering in Medicine and Biology Society. 6263–6266.

[100] K. Bhanu Prakash, V. Gupta, M. Bilello, N. J. Beauchamp, and W. L. Nowinski. 2006. Identification, Segmentation, and Image Property Study of Acute Infarcts in Diffusion-weighted Images by using a Probabilistic Neural Network and Adaptive Gaussian Mixture Model. *Academic Radiology*. 13: 1474–1484.